Supporting information for:

ESI-MS Study on First Generation Ruthenium Olefin Metathesis Catalysts in Solution: Direct Detection of the Catalytically Active 14-Electron Ruthenium Intermediate

Haoyang Wang and *Jürgen O. Metzger**

Institut für Reine und Angewandte Chemie, Carl von Ossietzky Universität, 26111, Oldenburg, Germany. E-mail: Juergen.Metzger@uni-oldenburg.de

1. ESI mass spectra of ruthenium catalyst 1 and 2.

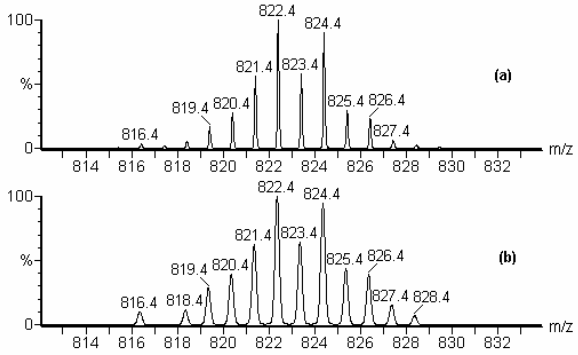

Figure S1. (a) Isotopic pattern of the ion $\mathbf{1}^{\bullet+}$; (b) theoretical isotopic pattern of the ion $\mathbf{1}^{\bullet+}$.

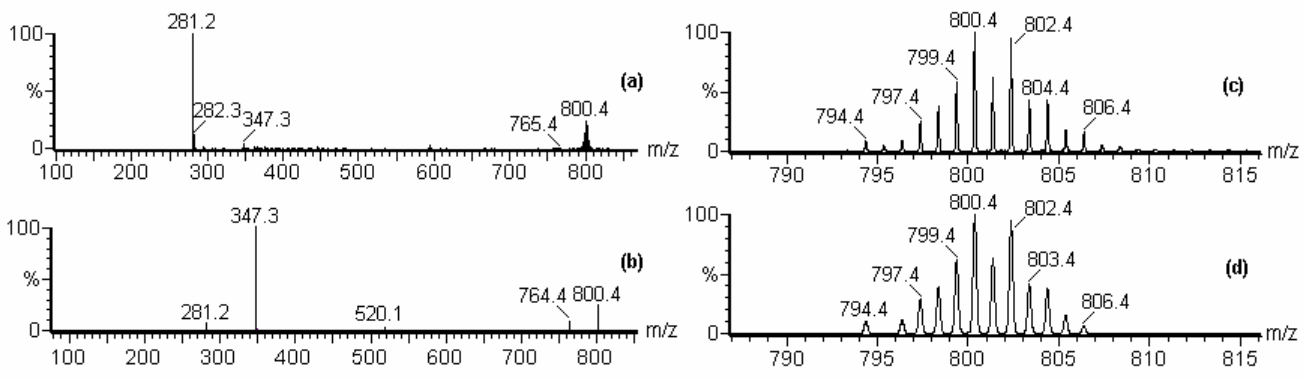

Figure S2. (a) ESI mass spectrum of the ruthenium catalyst **2**; (b) ESI-MS/MS spectrum for CID of $\mathbf{2}^{\bullet+}$; (c) isotopic pattern of the ion $\mathbf{2}^{\bullet+}$; (d) theoretical isotopic pattern of the ion $\mathbf{2}^{\bullet+}$.

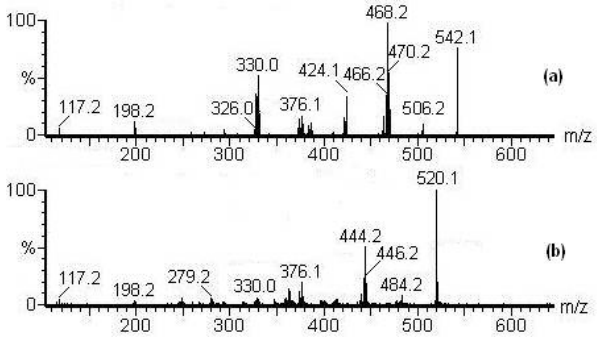

Figure S3. ESI-MS/MS spectra for CID of: (a) $\mathbf{1T}^{\bullet+}$at *m/z* 542.1; (b) $\mathbf{1T}^{\bullet+}$ at *m/z* 520

2. Phosphine exchange reactions of catalysts 1 or 2 with phosphine 3.

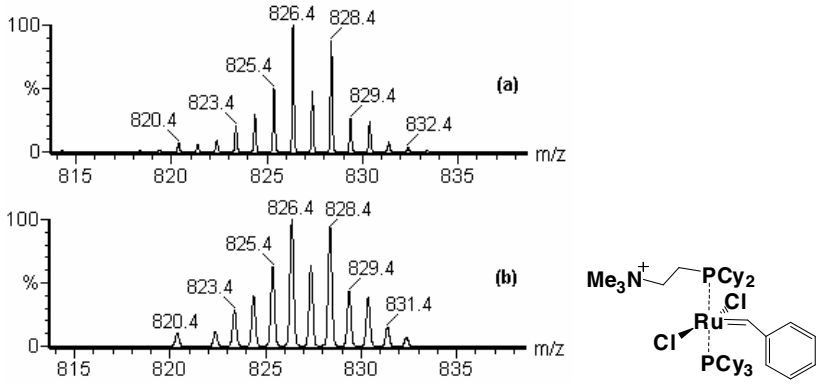

Figure S4. (a) Isotopic pattern of the ion **1A;** (b) theoretical isotopic pattern of the ion **1A.**

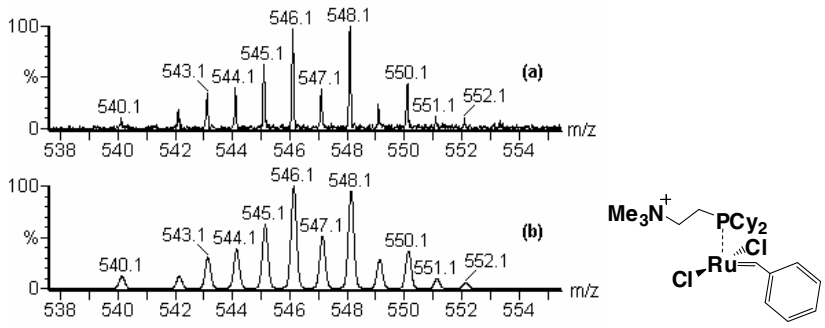

FigureS5. (a) Isotopic pattern of the ion **1B;** (b) theoretical isotopic pattern of the ion **1B.**

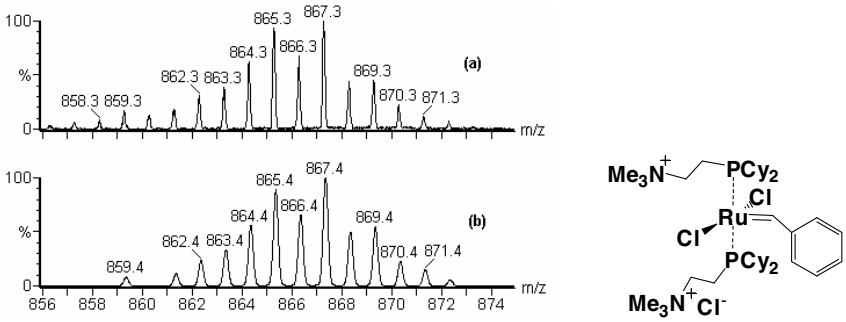

Figure S6. (a) Isotopic pattern of the ion **1C;** (b) theoretical isotopic pattern of the ion **1C.**.

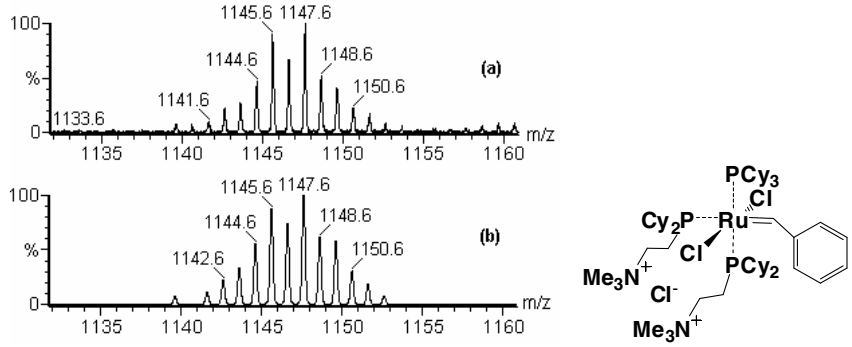

Figure S7. (a) Isotopic pattern of the ion **1D;** (b) theoretical isotopic pattern of the ion **1D.**

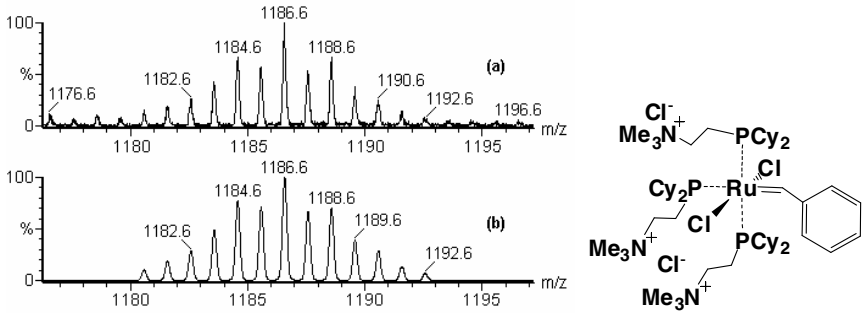

Figure S8. (a) Isotopic pattern of the ion **1E;** (b) theoretical isotopic pattern of the ion **1E.**

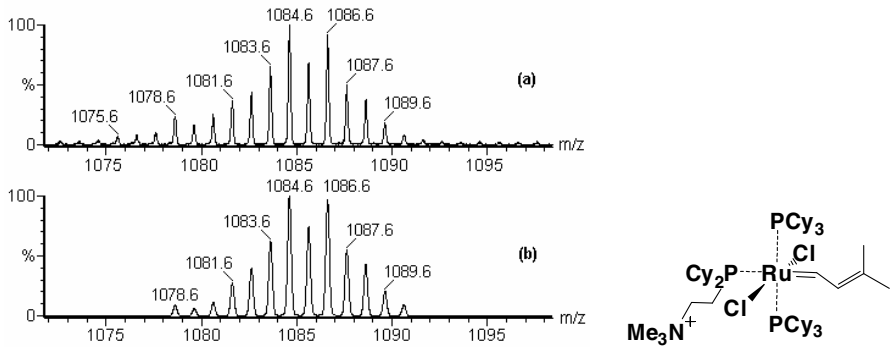

Figure S9. (a) Isotopic pattern of the ion **2F;** (b) theoretical isotopic pattern of the ion **2F.**

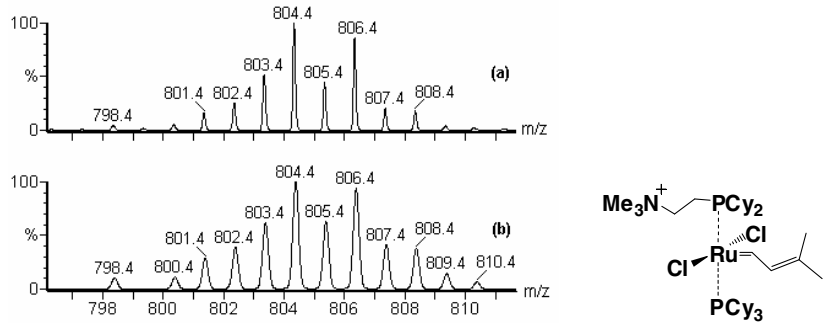

Figure S10. (a) Isotopic pattern of the ion **2A;** (b) theoretical isotopic pattern of the ion **2A.**

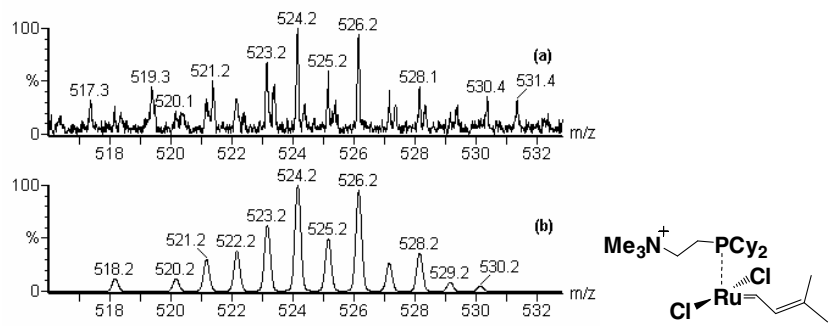

Figure S11. (a) Isotopic pattern of the ion **2B;** (b) theoretical isotopic pattern of the ion **2B.**

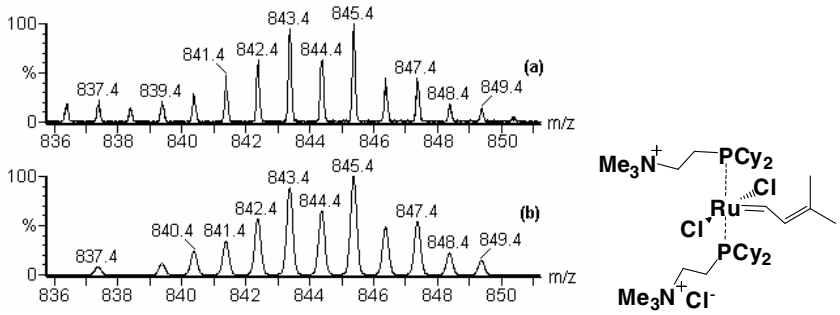

Figure S12. (a) Isotopic pattern of the ion **2C;** (b) theoretical isotopic pattern of the ion **2C.**

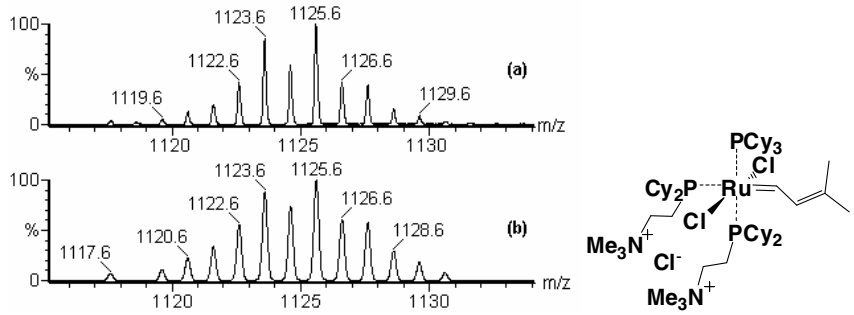

Figure S13. (a) Isotopic pattern of the ion **2D;** (b) theoretical isotopic pattern of the ion **2D.**

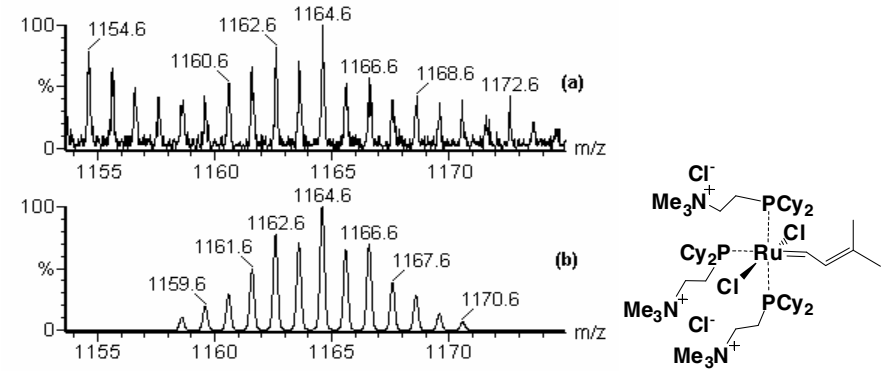

Figure S14. (a) Isotopic pattern of the ion **2E;** (b) theoretical isotopic pattern of the ion **2E.**

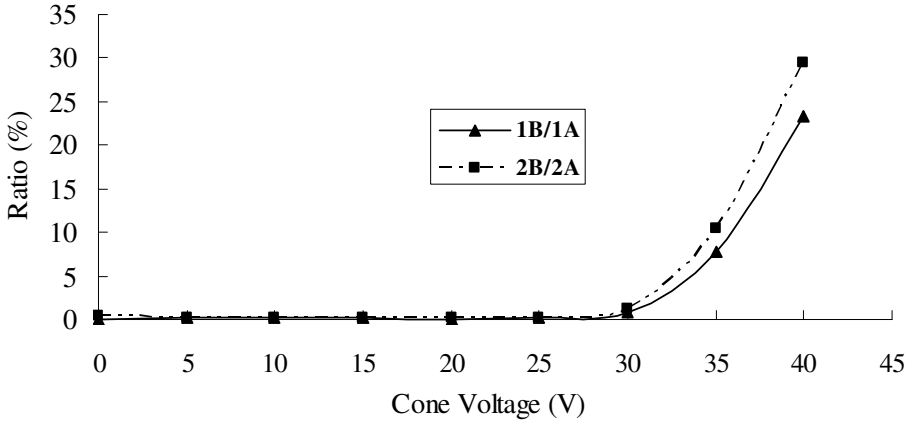

Figure S15. Dependence of the ratio of the intensitiy of the ions **1B:1A** and **2B:2A,** respectively, on the cone voltage.

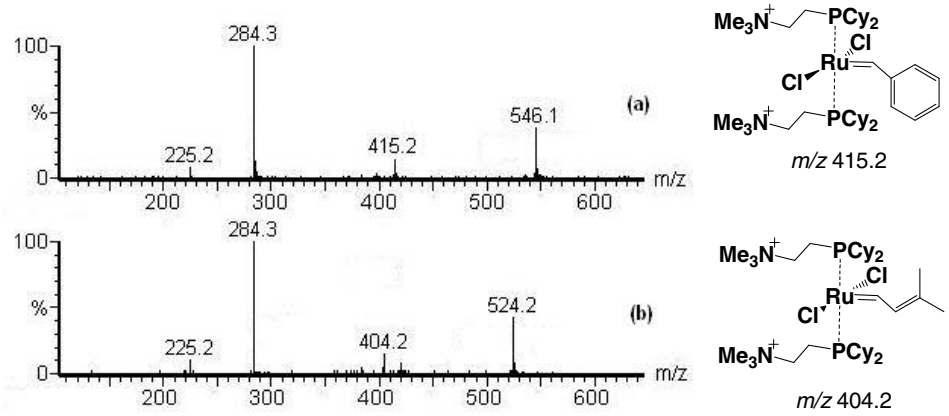

Figure S16. ESI-MS/MS spectra for CID of the double charged species: (a) **[1C**-Cl]$^{2+}$ at *m/z* 415; (b) [**2C**-Cl]$^{2+}$ at *m/z* 404.

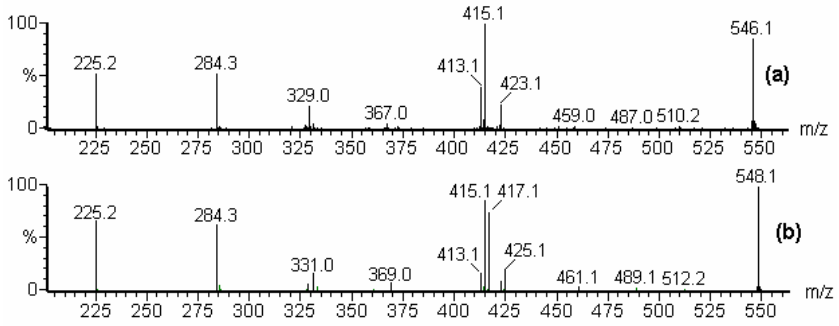

Figure S17. ESI-MS/MS spectra for CID of the isotopologues of the 14-electron ruthenium intermediate **1B** (a) the ion at *m/z* 546; (b) the ion at *m/z* 548 (fragmentation voltage 14eV).

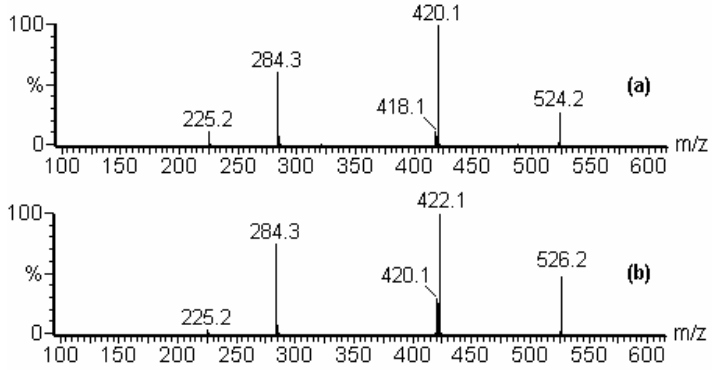

Figure S18. ESI-MS/MS for CID of the isotopologues of the 14-electron ruthenium intermediate **2B** at *m/z* 524 (a) the ion at *m/z* 524; (b) the ion at *m/z* 526 (fragmentation voltage 6eV)

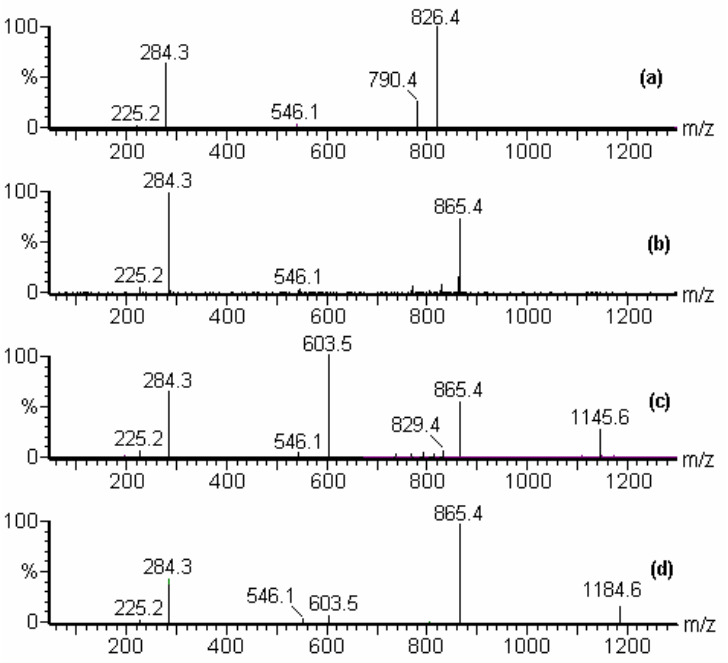

Figure S19. ESI-MS/MS spectra for CID of the ions: (a) **1A** at *m/z* 826; (b)**1C** at *m/z* 865; (c) **1D** at *m/z* 1145**;** (d) **1E** at *m/z* 1184

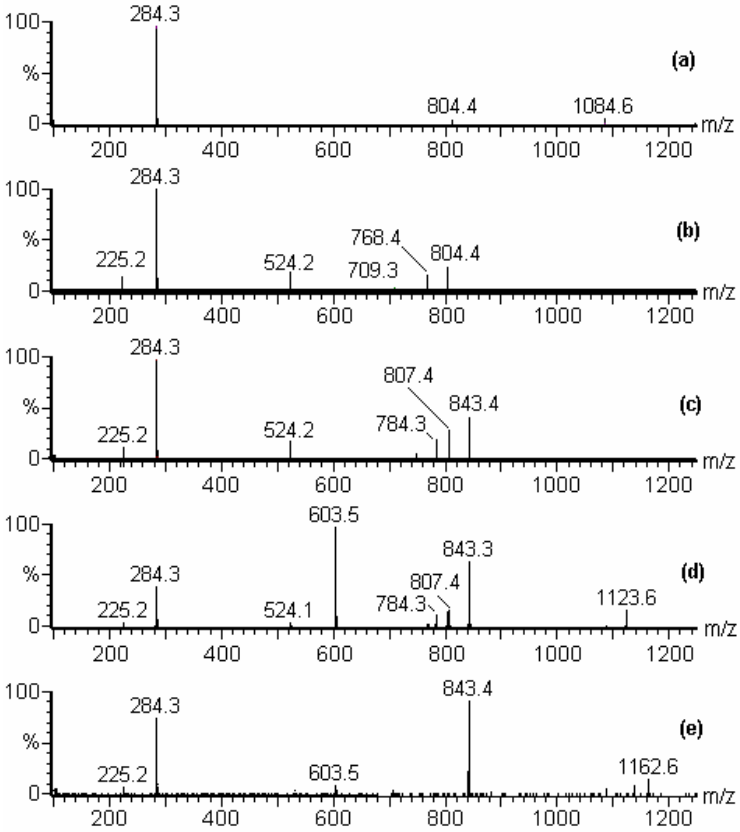

Figure S20. ESI-MS/MS spectra for CID of : (a) **2F** at *m/z* 1184; (b) **2A** at *m/z* 804; (c) **2C** at *m/z* 843; (d) **2D** at *m/z* 1123; (e) **2E** at *m/z* 1162

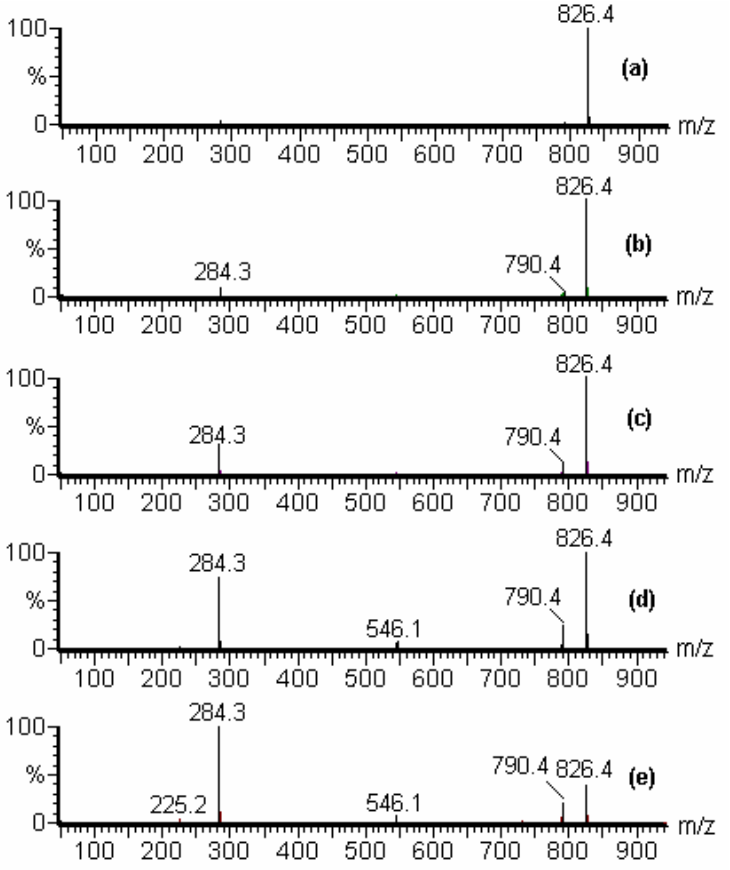

Figure S21. ESI-MS/MS spectra for CID of the ion **1A** at *m/z* 826 using increasing fragmentation voltages: (a) 0V; (b) 2V; (c) 4V; (d) 6V; (e) 8V.

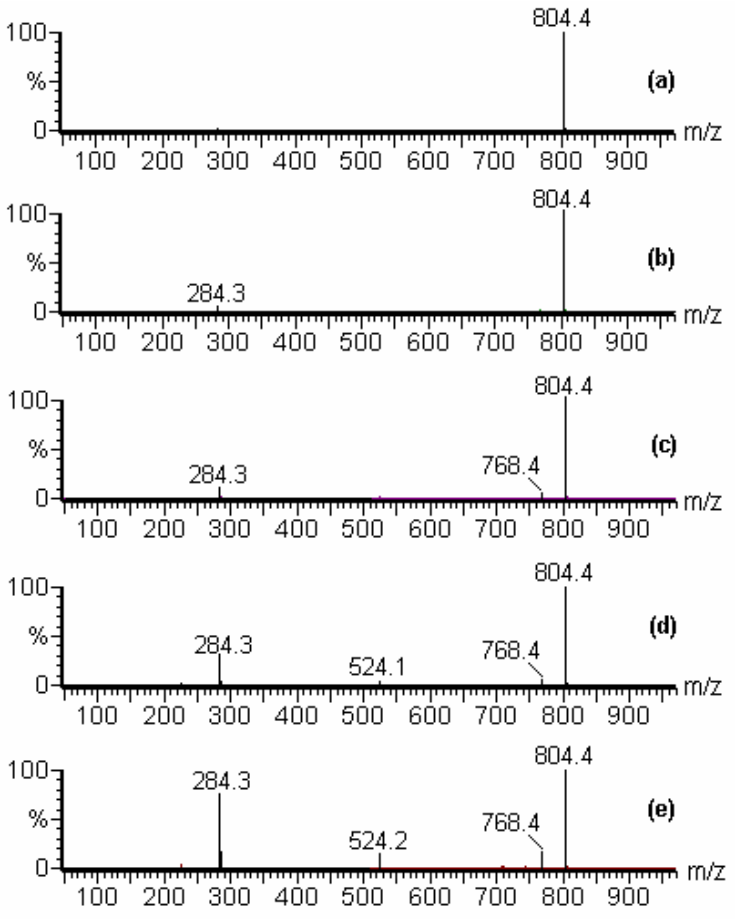

Figure S22. ESI-MS/MS spectra for CID of the ion **2A** at *m/z* 804 using increasing fragmentation voltages (a) 0V; (b) 2V; (c) 4V; (d) 6V; (e) 8V.

3. Directly monitoring the ring-closing metathesis reactions of dienes 5, 6 or 7 with catalyst 1.

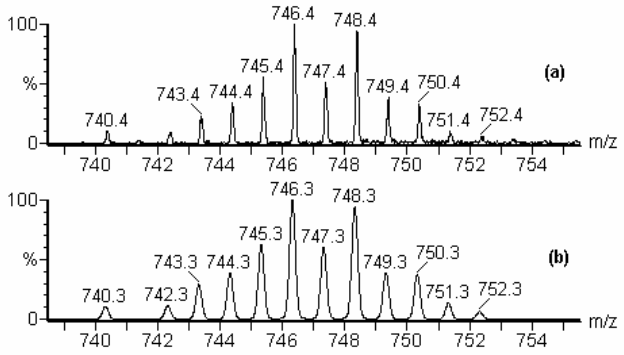

Figure S23. (a) Isotopic pattern of the ion $\mathbf{4}^{\bullet+}$**;** (b) theoretical isotopic pattern of the ion $\mathbf{4}^{\bullet+}$**.**

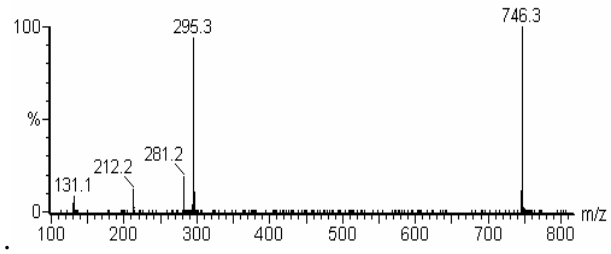

Figure S24. ESI-MS/MS spectrum for CID of: $\mathbf{4}^{\bullet+}$ at *m/z* 746.

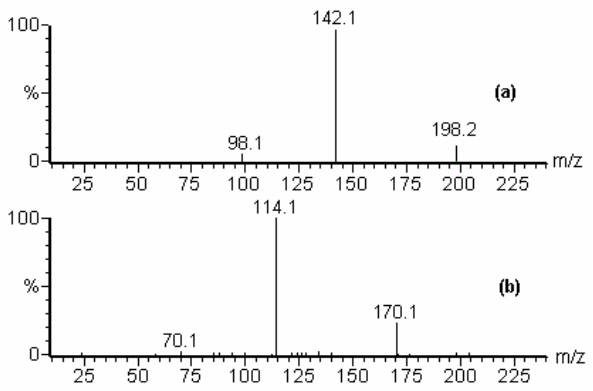

Figure S25. ESI-MS/MS spectra for CID of the protonated molecule of : (a) diene **5**; (b) product **8.**

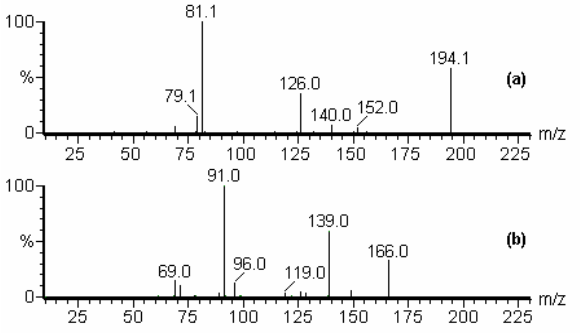

Figure S26. ESI-MS/MS spectra for CID of the protonated molecule of : (a) diene **6**; (b) product **9.**

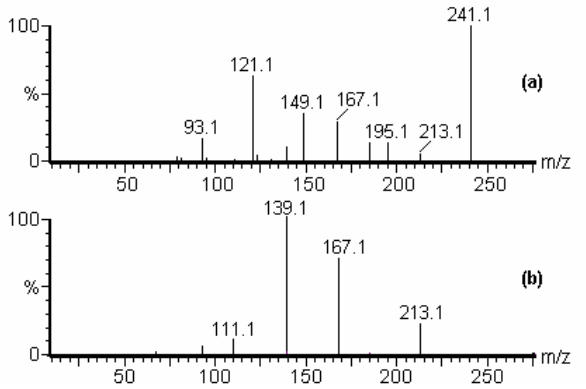

Figure S27. ESI-MS/MS spectra for CID of the protonated molecule of (a) diene **7**; (b) product **10.**

4. Directly monitoring the RCM reaction of dienes 5 with catalyst 1 in presence of 3·Cl

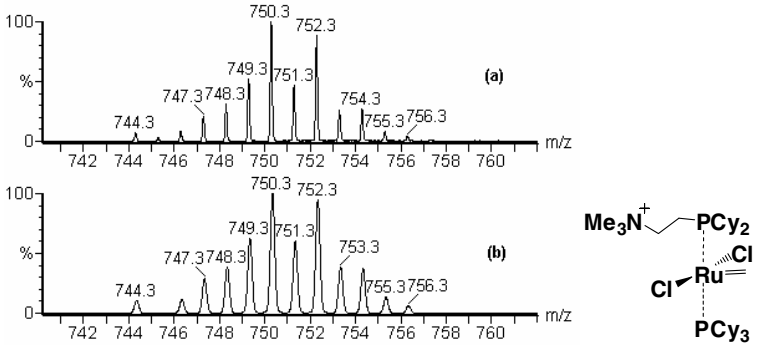

Figure S28. (a) Isotopic pattern of the ion **4A**; (b) theoretical isotopic pattern of the ion **4A**.

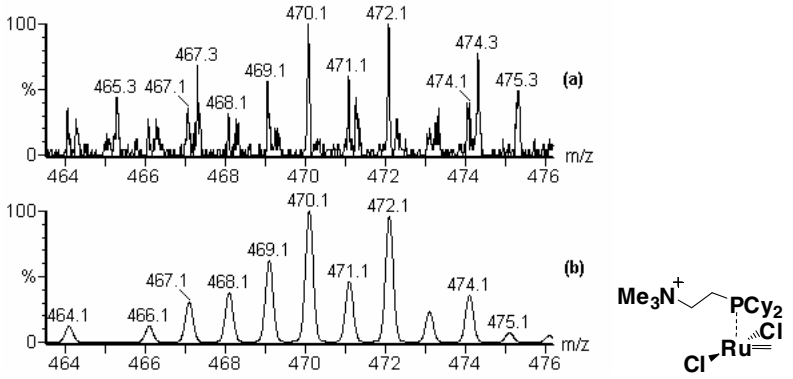

Figure S29. (a) Isotopic pattern of the ion **4B**; (b) theoretical isotopic pattern of the ion **4B**.

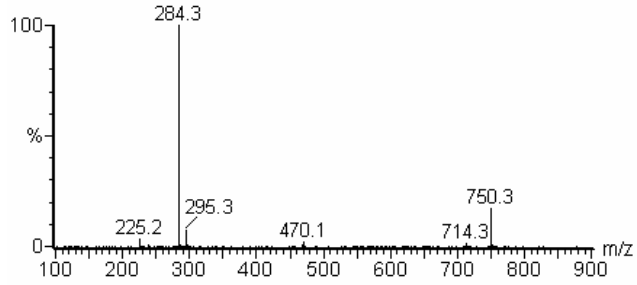

Figure S30. ESI-MS/MS spectrum for CID of the ion **4A** at *m/z* 750

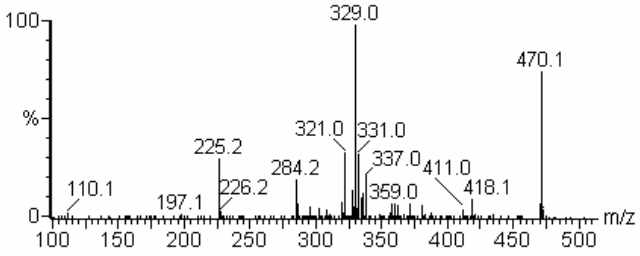

Figure S31. ESI-MS/MS spectrum for CID of the ion **4B** at *m/z* 470

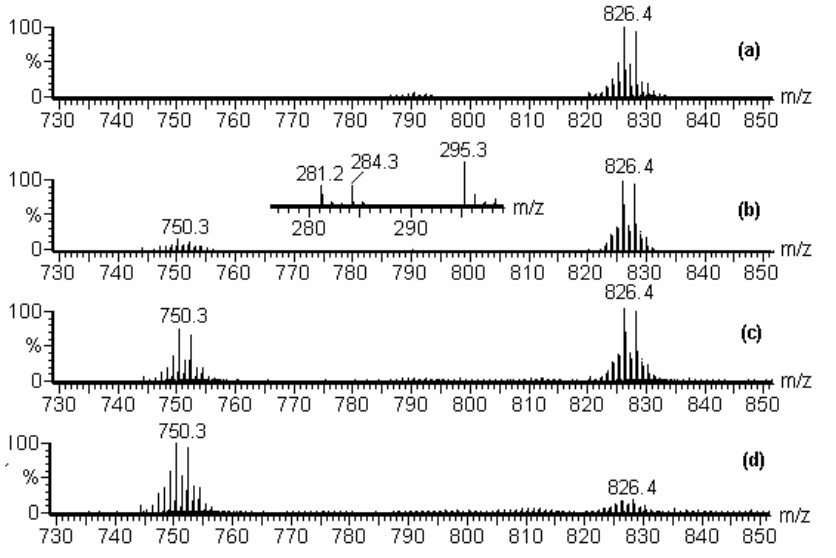

Figure S32. Expansion of ESI spectra of the ion species from the ring-closing metathesis reaction solution of **5** with **1** in presence of **3** at different time scale: (a) 0 second; (b) 6 second; (c) 12 second; (d) 2 minute. In the insert of figure S32b, the $CH_3P^+Cy_3$ at *m/z* 295 could be detected clearly in high abundance, as well as protonated PCy_3 at *m/z* 281 and **3** at *m/z* 284.

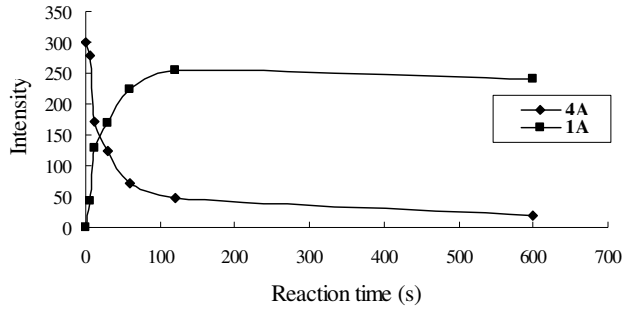

Figure S33. The changes of the intensity of **1A** and **4A** Vs. reaction time in ring-closing metathesis reaction of **5** with **1** in presence of **3**.

5. ESI detection of decomposition products of the catalysts: $PhCH_2P^+Cy_3$(11), CH_2=CCH_3CH=CHP^+Cy_3(12), $(CH_3)_3N^+CH_2CH_2P(Cy)_2$=Ph(13) and $CH_3P^+Cy_3$,

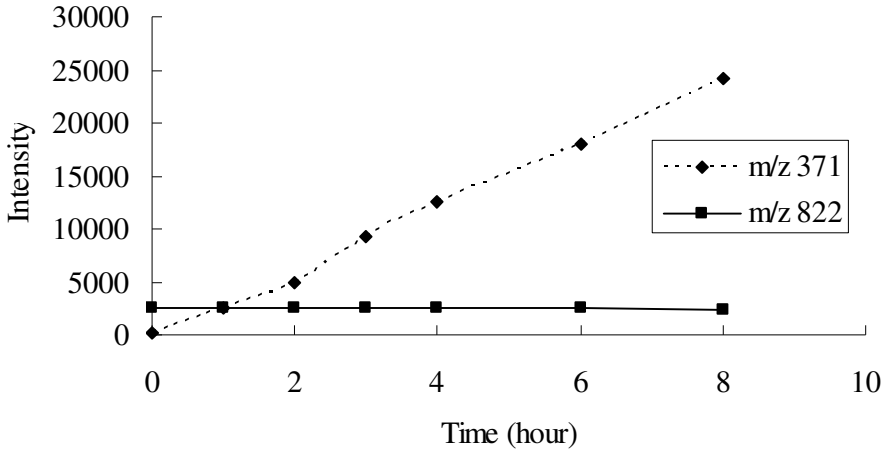

Figure S34. The changes of intensity of the decomposition product of **11** at *m/z* 371 and the radical cation of $\mathbf{1}^{\bullet+}$ at *m/z* 822 Vs. reaction time.

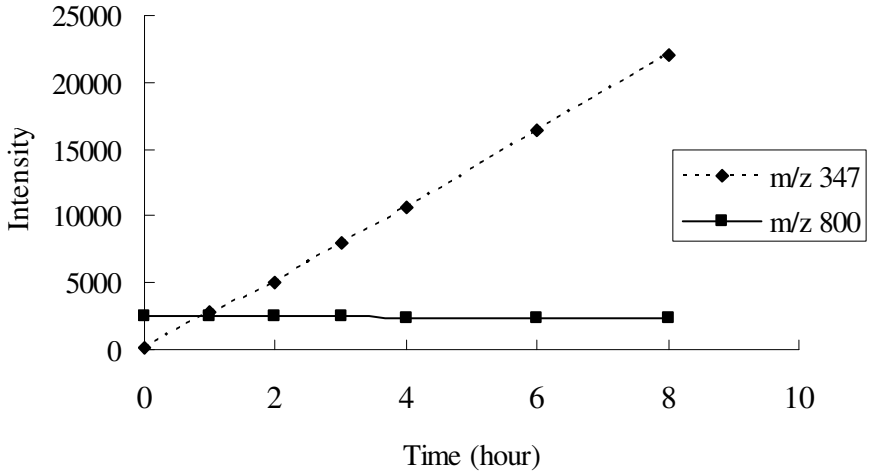

Chart S35. The changes of intensity of the decomposition product of **12** at *m/z* 347 and the radical cation of $\mathbf{2}^{\bullet+}$ at *m/z* 800 Vs. reaction time.

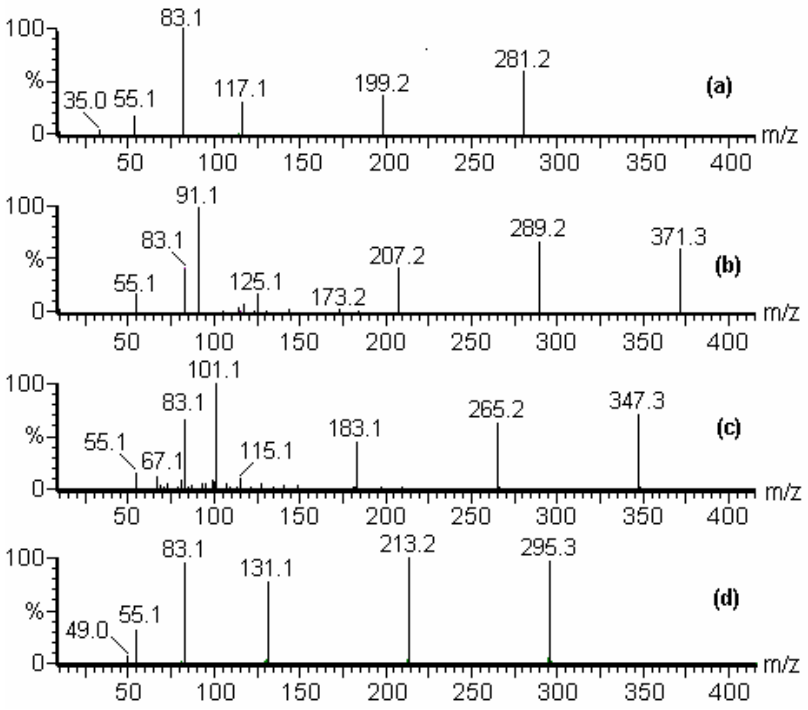

Figure S36. ESI-MS/MS spectra for CID of (a) $HP^{+}Cy_3$ at *m/z* 281; (b) $PhCH_2P^{+}Cy_3$ at *m/z* 371; (c) $CH_2{=}CCH_3CH{=}CHP^{+}Cy_3$ at *m/z* 347; (d) $CH_3P^{+}Cy_3$ at *m/z* 295

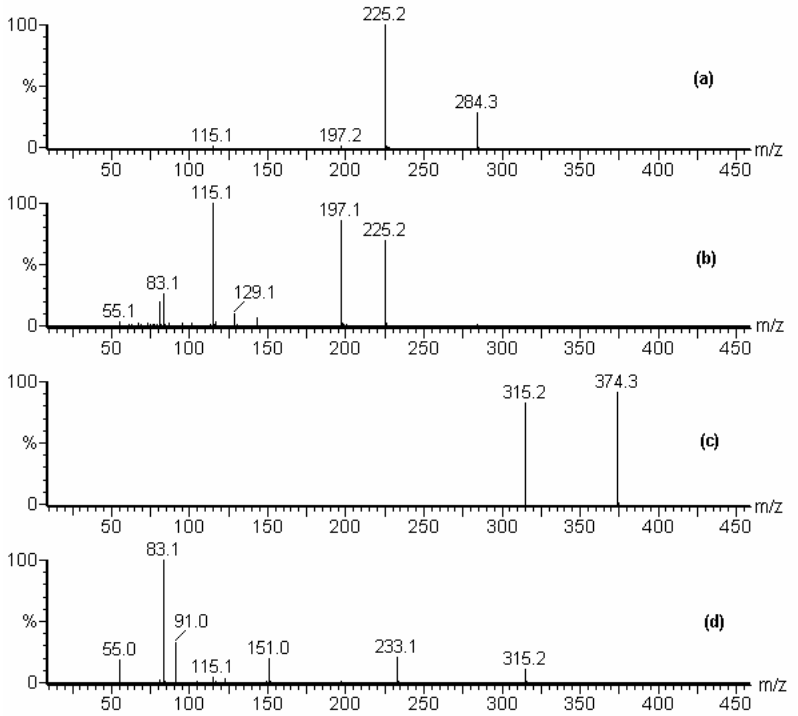

Figure S37. ESI-MS/MS spectra for CID of a) the ion **3** at *m/z* 284; b) the ion at *m/z* 225, generated by in-source CID from the ion **3**; c) the ion 1**3** at *m/z* 374; (d) the ion at *m/z* 315 , generated by in-source CID from the ion **13**.